TamperNN: Efficient Tampering Detection of Deployed Neural Nets

Erwan Le Merrer
Univ Rennes, Inria, CNRS, Irisa
erwan.le-merrer@inria.fr

Gilles Trédan
LAAS/CNRS
gtredan@laas.fr

Abstract

Neural networks are powering the deployment of embedded devices and Internet of Things. Applications range from personal assistants to critical ones such as self-driving cars. It has been shown recently that models obtained from neural nets can be *trojaned*; an attacker can then trigger an arbitrary model behavior facing crafted inputs. This has a critical impact on the security and reliability of those deployed devices.

We introduce novel algorithms to detect the tampering with deployed models, *classifiers* in particular. In the remote interaction setup we consider, the proposed strategy is to identify markers of the model input space that are likely to change class if the model is attacked, allowing a user to detect a possible tampering. This setup makes our proposal compatible with a wide range of scenarios, such as embedded models, or models exposed through prediction APIs. We experiment those tampering detection algorithms on the canonical MNIST dataset, over three different types of neural nets, and facing five different attacks (trojaning, quantization, fine-tuning, compression and watermarking). We then validate over five large models (VGG16, VGG19, ResNet, MobileNet, DenseNet) with a state of the art dataset (VGGFace2), and report results demonstrating the possibility of an efficient detection of model tampering.

1 Introduction

Neural network-based models are increasingly embedded into systems that take autonomous decisions in place of persons, such as in self-driving cars [28,36] or in robots [16]. The value of those embedded models is then not only due to the investments for research and development, but also because of their critical interaction with their environment. First attacks on neural-based classifiers [6] aimed at subverting their predictions, by crafting inputs that are yet still perceived by humans as unmodified. This leads to questions about the security of applications embedding them in the real world [17], and more generally initiated the interest of the security community for those problems [26]. Those *adversarial* attacks are confined in modifying the data inputs to send to a neural model. Yet, very recently, other types of attacks were shown to operate by *modifying the model itself*, by embedding information in the model weight matrices. This is the case of new *watermarking* techniques, that aim at embedding watermarks into the model, in order to prove model ownership [19, 23], or of *trojaning* attacks [4, 21] that empowers the attacker to trigger specific model behaviors.
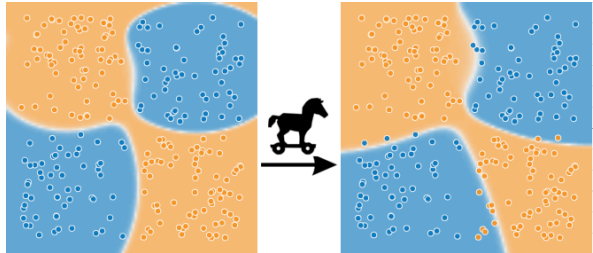

Figure 1: Illustration of a model tampering and its impact on the decision boundaries. We use the TensorFlow playground application for illustration; this toy dataset is fitted by a three hidden layer neural network (blue or yellow data inputs must be covered by their own color, ideally). The weights of solely the first layer have been modified (by removing -0.1 from them), to simulate an attack on the model. We observe slight changes of decision boundaries, that lead to misclassify some input data. This paper leverages such misclassifications for detecting the tampering attacks.

The fact that neural network weights are by them-

selves implicit (*i.e.*, they do not convey explicit behavior upon inspection as opposed to the source code or formal specification of a software component) expose applications to novel attack surfaces. It is obvious that those attacks will have increasingly important impact in the future, and that the model creators – such as companies – have a tremendous interest in preventing the tampering with their models, specially in embedded applications [28, 29].

In this context, we are interested in providing a first approach to detect the tampering of a neural network-based model that is deployed on a device by the model creator. We stress that one can consider as an attack *any* action on a model (*i.e.*, on its weights) that was not performed by the creator or the operator of that model. To illustrate the practical effect of the tampering with a model, we present in Figure 1 a scenario of a fitted model (leftmost image) over two classes of inputs (blue and yellow dots). After a slight manipulation of few weights of the model (attack described in the Figure caption), we can observe the resulting changes in the model decision boundaries on the rightmost image. The attack caused a movement of boundaries, that had the consequence at inference time to return some erroneous predictions (*e.g.*, blue inputs in the yellow area are now predicted as part of the wrong class). Those wrong predictions might cause safety issues for the end-user, and are thus due to the attack on the originally deployed model.

1.1 Practical illustration of an attack: a trojaned classifier

We motivate our work through a practical attack, using the technique proposed by Liu et al. in [21]. The goal of the attack is to inject a malicious behaviour into an original model, that was already trained and was functional for its original purpose. The technique consists in generating a *trojan trigger*, and then to retrain the model with synthesized datasets in order to embed that trigger into the model. The trigger is designed to be added to a benign input, such as an image, so that this new input triggers a classification into the class that was targeted by the attacker. This results in a biased classification triggered on demand, with potentially important security consequences. The model is then made available as an online service or placed onto a compromised device; its behavior facing user requests appears legitimate. The attacker triggers the trojan at will by sending to the model an input containing the trojan trigger.

A face recognition model, known as the VGG Face model [27], has been trojaned with the technique in [21] and made available for download [5] by the authors of the attack. We access both this model and its original version. The observed modifications in the weights do not indicate, a priori, to which extent the accuracy has been modified (as depicted in Figure 1 where blue inputs get the orange label and vice-versa), as neural-based models have highly implicit behaviours. One then has to pass a test dataset through the classification API to assess the accuracy change. The authors report an average degradation of only 2.35% over the original test data, for the VGG Face trojaned model. In other words, both models exhibit a highly similar behaviour (*i.e.*, similar classifications) when facing benign inputs. As a countermeasure to distinguish both models, an approach is compute such a variation or, in a more straightforward approach, to compute hashes of their weights (or hashes of the memory zone where the model is mapped) and to compare them [10]. However, this approach requires a direct access to the model.

Unfortunately, models are not always (easily) accessible, because of their embedding on IoT like devices for instance, as reported in work by Roux et al. [29]. This accessibility problem arises in at least in two contexts of growing popularity: *i*) if the model is directly embedded on a device and *ii*) if the model is in production on a remote machine and only exposed through an API. In such cases where the model is only accessible through its query API, one can think about a black-box testing approach [7]: it queries the suspected model with specific inputs, and then compares the outputs (the obtained classification labels) with those produced by the original model.

In this paper, we study the efficiency of novel black-box testing approaches. Indeed, while in theory testing the whole model input space would for sure reveal any effective tampering, this would require an impractical amount of requests. For this approach to be practical, the inputs used for querying the model shall be chosen wisely. Our core proposal is then to identify specific inputs whose property is to change classification as soon as the model is tampered with. We refer to these crafted inputs as *markers*. Our research question is: *How to craft sets of markers for efficient model tampering detection, in a black-box setup?*

2

1.2 Considered setup: black-box interactions

While there exists a wide range of techniques, at the system or hardware level, to harden the tampering with software stacks on a device (please refer to the Related Work Section), the case of neural network models is salient. Due to the intrinsic accuracy change of the model accuracy after the attack (cf Figure 1), we argue that stealthy, lightweight, and application-level algorithms can be designed in order to detect attacks on a remotely executed model.

We consider the setup where a *challenger*, possibly a company that has deployed the model on its devices, queries a *remote* device with standard queries for classifying objects. This is possible through the standard classification API that the device exposes for its operation (paper [34] discusses the same query setup for classification APIs of web-services). To a query with a given input object (*e.g.*, image, sound file) is answered (inferred) a class label among the set of classes the model has been trained for; this is the nominal operation of a neural classifier. Note that for maximal applicability, we do not assume that the device is returning probability vectors along with classes; such an assumption would make the problem easier, but also less widely applicable (as it is known from previous attacks for stealing models that those probabilities should *not* be returned, for security hardening facing attackers attempts [30, 34]).

1.2.1 Contributions

The contributions of this paper are:
(i) to introduce the problem of the tampering detection of neural networks in the back-box setup, and to formalize this problem in Section 2.
(ii) to propose three algorithms to address the challenge of efficient detection, by crafting markers that serve as attack witnesses. Those are compared to a strawman approach. Each have their own scope and efficiency on certain types of neural networks facing different attacks.
(iii) to extensively experiment those algorithms on the canonical MNIST dataset, trained on three state of the art neural network architectures. We do not only consider the attack of trojaning, but also generalize to any attempt to modify the weights of the remote neural network, through actions such as fine-tuning, compression, quantization, and watermarking. We then validate the efficiency of our approach over five large public models, designed for image clas-

sification (VGG16, VGG19, ResNet, MobileNet and DenseNet).

1.2.2 Organization of the paper

The remaining of this paper is organized as follows. We first precisely define the black-box interaction setup in the context of classification, and define the tampering detection problem in that regard in Section 2. The algorithms we propose are presented in Section 3, before they are experimented with in Section 4; the limits of the black-box setup for tampering detection are also presented in that Section. We finally review the Related Work in Section 5 and conclude in Section 6.

2 Design rationale

2.1 The black-box model observation setup

We study neural network classifiers, that account for the largest portion of neural network models. Let d be the dimensionality of the input (feature) space X, and C the set of target labels of cardinality $n = |C|$. Let $\mathcal{M} : \mathbb{R}^d \to C$ be a classifier model for the problem[1], that takes inputs $x \in X$ to produce a label $\hat{y} \in C$: $\mathcal{M}(x) = \hat{y}$.

To precisely define the notion of decision boundary in this context we need the posterior probability vector estimated by $\mathcal{M}$: $\{\mathbb{P}(c|x, \mathcal{M}), c \in C\}$. When the context is clear we will omit x and $\mathcal{M}$ to simply write $\mathbb{P}(c)$. Note that while internally $\mathcal{M}$ needs to generate this vector to produce its estimate $\hat{y} = \arg\max_{c \in C}(\mathbb{P}(c))$, we assume a black-box observation where only $\hat{y}$ is available to the user.

Definition 1 (Black-box model). *The challenger queries the observed model $\mathcal{M}$ with arbitrary inputs $x \in X$, and gets in return $\mathcal{M}(x) = \hat{y} \in C$.*

This setup is strictly more difficult than a popular setup where the probability vector is made available to the user (but that can lead to misuses, as shown in in [34] by "stealing" the remote model).

We now give a definition of the decision boundary of a model. This definition is adapted from [20] for the black-box setup.

---

[1]By *model*, we mean the trained model from a deep neural network architecture, along with its hyper-parameters and resulting weights.

Definition 2 (Decision boundary). *Given $\mathcal{M}$, an input $x \in X$ is on the decision boundary between classes if there exists at least two classes $c_i, c_j \in C$ maximising the posterior probability: $\mathbb{P}(c_i) = \mathbb{P}(c_j) = \max_{c \in C} \mathbb{P}(c)$.*

The set of points on decision boundaries defines a partitioning of input space X into C equivalence classes, each class containing inputs for which $\mathcal{M}$ predicts the same label.

We can now provide the definition of models distinguishability when queried in a black-box setup, based on the returned labels.

Definition 3 (Models distinguishability). *Two models $\mathcal{M}$ and $\mathcal{M}' \neq \mathcal{M}$ can be distinguished in a black-box context if and only if $\exists \ x \in X$ s.t. $\mathcal{M}(x) \neq \mathcal{M}'(x)$.*

Note that this implies that their decision boundaries are not equivalent on input space X. Conversely, two different classifiers that end up through a training configuration to raise the same decision boundaries on input space X, with equivalent classes in each region, are *indistinguishable* from an observer in the black-box model.

Indistinguishability is trivially the inability to distinguish two models. Since it is generally impossible to test the whole input set X, a restricted but practical variant is to consider the indistinguishability of two models with regards to a given set of inputs, α. We name this variant α-*set indistinguishability*.

Since we are interested in cases where $\mathcal{M}'$ is a slight alteration of the original model $\mathcal{M}$, it is interesting to quantify their differences over a given set S:

Definition 4 (Difference between models). *Given two models $\mathcal{M}$, $\mathcal{M}'$ and a set S, the difference between $\mathcal{M}$ and $\mathcal{M}'$ on S is defined as: $\Delta(\mathcal{M}, \mathcal{M}', S) = \frac{1}{|S|} \cdot \sum_{x \in S} \delta(\mathcal{M}(x), \mathcal{M}'(x))$, with $\delta(.) = 1$ if $\mathcal{M}(x) \neq \mathcal{M}'(x)$, 0 otherwise.*

In this light, two S-set indistinguishable models $\mathcal{M}$ and $\mathcal{M}'$ have by definition $\Delta(\mathcal{M}, \mathcal{M}', S) = 0$.

Definition 5 (Model stability). *Given an observation interval in time $\mathcal{I} = [t_0, t_e]$, and a model $\mathcal{M}$ observed at time t_0 (noted $\mathcal{M}_{t_0}$), the model $\mathcal{M}$ is stable if it is indistinguishable from $\mathcal{M}_{t_0} \forall t \in \mathcal{I} \setminus t_0$.*

2.2 The problem of tampering detection

Problem 1 (Tampering detection of a model in the black-box setup). *Detect that model is not stable, according to Definition 5.*

This means that finding one input x so that $\mathcal{M}_{t_0}(x) \neq \mathcal{M}_{t'}(x)$ is sufficient to solve Problem 1. Consequently, an *optimal* algorithm for solving Problem 1 is an algorithm that provides, for any model $\mathcal{M}$ to defend, a *single* input that is guaranteed to see its classification changed on the attacked model $\mathcal{M}'$, for any possible attack.

Since it is very unlikely, due to the current understanding of neural networks, to find such an optimal algorithm, we resort to finding sets of markers (specific data inputs) whose likelihood to change classification is high as soon as the model is tampered with. Since the challenge is to be often executed, and be as stealthy as possible, we refine the research question: *Are there algorithms to produce sensitive and small marker sets allowing model tampering detection in the black-box setup?* More formally, we seek algorithms that given a model $\mathcal{M}$ find sets of inputs $K \subset X$ of low cost and high sensitivity to attacks:

Definition 6 (Tampering detection metrics).

- *Cost: $|K|$, the number of requests needed to evaluate $\{\mathcal{M}(x), \forall x \in K\}$.*

- *Sensitivity: The probability to detect any model tampering, namely that at least one input (marker) of K gets a different label. Formally, the performance of a set K can be defined as $\mathbb{P}(\exists x \in K \text{ s.t. } \mathcal{M}(x) \neq \mathcal{M}'(x), \forall \mathcal{M}')$.*

It is easy to see that both metrics are bound by a tradeoff: the bigger the marker set, the more likely it contains a marker that will change if the model is tampered with. We now have a closer look to this relation.

2.2.1 Cost-sensitivity tradeoff

As stated in the previous Section, we assume in this paper that the remote model returns the minimal information, by building our algorithms with solely labels being returned as answers ($\mathcal{M}(x) \in C$).

Let $\mathcal{M}$ an original model, and $\mathcal{M}'$ a tampered version of $\mathcal{M}$. Consider a set of inputs $K \subset X$ of cardinality (cost) s. Let $p = \mathbb{P}(\mathcal{M}(x) \neq \mathcal{M}'(x))$ be the probability that a marker $x \in K$ triggers (that is, x allows the detection of the tampering). In the experiments, we refer to estimations of p as the *marker triggering ratio*. Assume that given a model tampering the probabilities of each marker to trigger are

independent. The overall probability to detect the tampering by querying with K of size s is the sensitivity $c = 1 - (1 - p)^s$. While the challenger is tempted to make this probability as high as possible, he also desires to keep s low to limit the cost of such an operation, and to remain stealthy.

In general, we assume the challenger first fixes the desired sensitivity c as a confidence level of his decisions (say for instance 99% confidence, $c = .99$). It turns out that one can easily derive the minimum key size s given p and c:

$$(1-p)^s < 1 - c$$
$$s \times log(1-p) < log(1-c)$$
$$s > log(1-c)/log(1-p)$$

These relations highlight the importance of having a high marker triggering ratio: there is an exponential relation between p and s. This relation is illustrated Figure 2, that relates the key size s, the marker triggering ratio, and the chosen confidence. Please note the inverted logscale on the y-axis. It shows that for a constant confidence $c = .99$ (dashed line), a key composed by markers easily triggered will be small (*e.g.*, 6 for $p = 0.5$), while a key composed by markers with a low trigger ratio will be considerably larger (458 for $p = 0.01$ for instance).

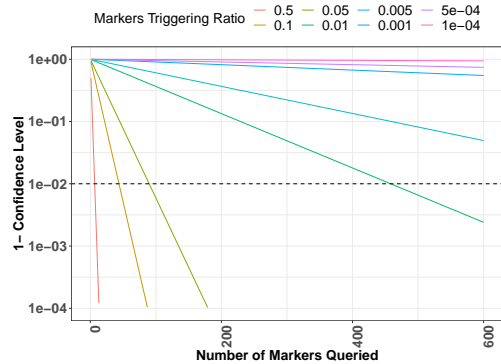
Figure 2: y-axis: Inverse Confidence Level for (*i.e.*, probability of failing at) detecting a tampered model, with the amount of queries on the x-axis, and for a given marker triggering ratio (indicated on the top legend).

This short analysis is stressing the importance of designing efficient algorithms that craft markers which have a high chance to be misclassified after the attack; this permits to challenge the model with less markers.

Finally, let us note that the goal of an attacker, beside the successful implementation of his attack (*e.g.*, the embedding of the trojan trigger in the method proposed in [21]), is to have the minimal impact on the model accuracy for obvious stealthiness reasons (*e.g.*, the claim for only 2.35% degradation in [21]). We thus have the classical conflicting interests for the attacker and the challenger: the challenger hopes for a noticeable attack in order to detect it more easily, while the attacker leans towards the perfect attack leaving no trace at all. This motivates the research for the crafting of very sensitive markers, in order to detect even the slightest attacks on a model.

3 Algorithms for the Detection of Remote Model Tampering

3.1 Reasoning facing black-box model classifications

Since we aim at leveraging a limited set of marker queries to challenge the model, and because success probability is involved, let us introduce notions of true and false positives for Problem 1. A true positive refers to a tampered model being detected as such, a true negative corresponds to the legitimate (original) model being recognized as original.

3.1.1 False negatives in tampering detection

Regarding the problem of tampering detection in the black-box setup, a false negative for the detection occurs if an algorithm challenges the model, gets classifications, and concludes that the model has not been tampered with, while it was actually the case. The probability of failure that we presented in Figure 2 thus constitutes the probability of false negatives.

3.1.2 False positives in tampering detection

In this setup, assuming that the original model has a deterministic behaviour, false positives cannot happen. A false positive would be the detection of an attack that did not occur. Since the challenger had full control over his model before deployment, he knows the original labels of his markers. Any change in those labels is by the problem definition an indication of the tampering and therefore cannot be misinterpreted as an attack that never occurred.

3.2 The strawman approach and three algorithms

The purpose of the novel algorithms we are now presenting is to provide the challenger with a key K to query the remote model, that is composed of a set of $|K| = s$ input markers. Concretely, given an original model $\mathcal{M}$, those algorithms generate a set of markers K. The owner of the model stores K along with the response vector $\hat{Y}_{\mathcal{M}}$, associated with the markers in K: $\hat{Y}_{\mathcal{M}} \leftarrow \mathcal{M}(i), \forall i \in K$.

We assume that K is kept secret (unknown to the attacker). When the user needs to challenge a potentially attacked model $\mathcal{M}'$, it simply queries $\mathcal{M}'$ with inputs in K, and compares the obtained response vector $\hat{Y}_{\mathcal{M}'}$ with the stored $\hat{Y}_{\mathcal{M}}$. If the two response vectors differ, the user can conclude that $\mathcal{M} \neq \mathcal{M}'$.

The algorithms are designed to operate on widely different aspects of black-box model querying. Table 1 synthesizes the different knowledge exploited by those algorithms. Cases where the remote model is accessible (*i.e.*, white-box testing) can be solved by direct weight comparison or standard software integrity testing approaches [10], and are not in the scope of this paper.

SM (standing for *strawman*) represents an intuitive approach, consisting in tracking a sort of "non-regression" with regards to the initial model deployed on devices. The GRID algorithm (*grid-like inputs*) is also model agnostic, as it generates inputs at random, that are expected to be distant from real-data distribution, and then to assess boundary changes in an efficient way. Both WGHT (*perturbation of weights*) and BADV (*boundary adversarial examples*) take as arguments the model to consider, and a value ϵ; the former applies a random perturbation on every weight to observe which are the most sensitive inputs with regards to misclassification after the attack (in the hope that those inputs will also be sensitive to forthcoming attacks). The latter generates *adversarial* inputs by the decision boundaries, in the hope to be sensitive to their movements. We now give their individual rationale in the following subsections, and present in Figure 3 an illustration.

3.2.1 The strawman approach (SM)

This strawman approach uses inputs from the test set as markers in order to assess changes in classification. An initial classification is performed for the markers before model deployment, and the resulting classes are expected to remain identical in subsequent
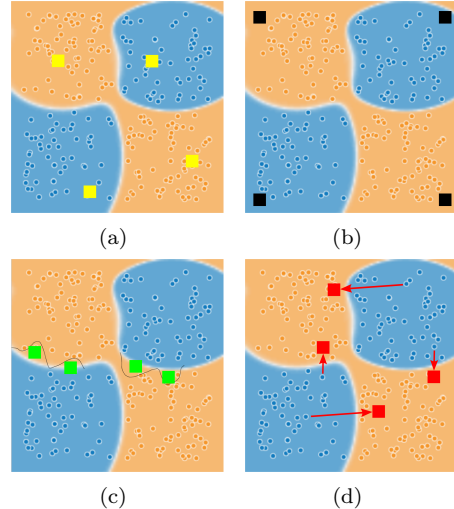

(a)   (b)

(c)   (d)

Figure 3: The placement of markers by the four algorithms. SM (a) picks a fraction of the test set inputs as markers; their position are thus related to the position of the dataset inputs. GRID (b) places markers at random corners of the d dimensional hyper-cube delimiting the input space. WGHT (c) finds inputs of the test set that are sensitive to weight perturbations, to select them as markers. Finally, BADV (d) converts test set inputs into adversaries located nearby the boundaries.

Algorithm 1: SM

Input: A test set $\mathcal{T}$; s

1 for 0 **to** s **do**
2 | $K.append(\mathcal{T}[\text{random\_int}(|\mathcal{T}|)])$
3 end
4 return K

---

queries.

Algorithm 1 then simply returns a key of size s, from the random selection of inputs in the provided test set $\mathcal{T}$.

3.2.2 Grid-like inputs (GRID)

This algorithm generates markers independently of the model $\mathcal{M}$ that is to be challenged.

Most generally, in classification tasks, the inputs are normalized before their usage to train the model. Without loss of generality for a normalization out of the $[0, 1]$ range, for each of the d dimensions of the considered model (*e.g.*, the 784 dimensions of a MNIST image), Algorithm 2 sets a random bit. The rationale is to generate markers that are far apart the

	Input format	A bunch of inputs	Original weights	Original architecture	Remote weights
Remote Opacity	Black-Box				White-Box
Original Opacity	Black-Box		White-Box		
Knowledge Required	Input format	A bunch of inputs	Original weights	Original architecture	Remote weights
Algorithm	GRID	SM	WGHT	BADV	–

Table 1: Summary of Algorithm requirements, ordered by the amount of knowledge required for the challenge.

Algorithm 2: GRID

Input: Image width x and height y; s

```
1  for 0 to s do
2      for 0 to x do
3          for 0 to y do
4              img[x][y] ← random_bit()
5          end
6      end
7      K.append(img)
8  end
9  return K
```

Algorithm 3: WGHT

Input: A test set $\mathcal{T}$; a model $\mathcal{M}$; a small ϵ; s

```
1   for i ← 0 to |T| do
2       pre.append(M(i))
3   end
4   for i ← 0 to |get_weights(M)| do
5       M.set_weight(i, M.get_weight(i) +
            random_float(−ε, +ε))
6   end
7   for i ← 0 to |T| do
8       post.append(M(i))
9   end
10  for i ← 0 to s do
11      if pre(i) ≠ post(i) then
12          K.append(pre(i))
13      if |K| = s then
14          break;
15  end
    /* Assumes |K| = s, increase ε otherwise    */
16  return K
```

Algorithm 4: BADV

Input: A test set $\mathcal{T}$; a model $\mathcal{M}$; an attack $\mathcal{A}$; a small ϵ; s

```
1   for i ← 0 to |T| do
2       adv.append(A(M(i), ε))
3       if M(i) ≠ M(adv) then
4           K.append(adv)
5       if |K| = s then
6           break;
7   end
    /* Assumes |K| = s, increase ε otherwise    */
```

---

actual probability distribution of the base dataset: since the training and tampering with $\mathcal{M}$ are willing to preserve accuracy, constraints are placed on minimizing test set misclassification. The consequence is a large degree of freedom for decision boundaries that are far apart the mass of inputs from the training set. We thus expect those crafted inputs to be very sensitive to the movement of boundaries resulting from the attack.

3.2.3 Perturbation of weights (WGHT)

The WGHT algorithm takes as arguments the model $\mathcal{M}$, and a value ϵ. It observes the classifications of inputs in dataset $\mathcal{T}$, before and after a perturbation has been applied to all weights of $\mathcal{M}$ (*i.e.*, a random perturbation of every weight to up to $\pm\epsilon$). Inputs for which label have changed, due to this form of tampering, are sampled to populate key K. The rationale is that with a low ϵ, the key markers are expected to be very sensitive to the tampering of model $\mathcal{M}$. In other words, inputs from K are expected to be the most sensitive inputs from $\mathcal{T}$ when it comes to tamper with the weights of $\mathcal{M}$.

3.2.4 Boundary adversarial examples (BADV)

Adversarial examples have been introduced in the early works presented in [6] and re-framed in [33], in order to fool a classifier (by making it misclassify inputs) solely due to slight modifications of the inputs. Goodfellow et al. then proposed [11] an attack for applying perturbations to inputs that leads to vast misclassifications of the provided inputs (that attack is named the *fast gradient sign attack or FGSM*). Those crafted inputs yet appear very similar to the original ones to humans, which leads to important security concerns [28]; note that since then, many other attacks of that form were proposed (even based on different setup assumptions [24]), as well as platforms to generate them (*e.g.*, [1] or [2]).

We propose with BADV to leverage the FGSM attack, but in an adapted way. The FGSM attack adds the following quantity to a legitimate input x: $\epsilon \times sign(\nabla_x J(\mathcal{M}, x, y))$, with ∇_x being the gradient

of J (the cost function used to train model $\mathcal{M}$), and y the label of input x. ϵ captures the intensity of the attack on the input. Approach in [11] is interested in choosing an ϵ that is large enough so that most of the inputs in the batch provided to the FGSM algorithm are misclassified (*e.g.*, $\epsilon = 0.25$ leads to the misclassification of 97.5% of the MNIST test set). We are instead interested in choosing an ϵ that is sufficient to create s misclassified markers only; the rationale is that the lower the ϵ, the closer the crafted inputs are to the decision boundary; our hypothesis is that this proximity will make those inputs very sensitive to any attack of the model that will even slightly modify the position of decision boundaries. In practice, and with Algorithm 4, we start from a low ϵ, and increase it until we get the desired key length s.

4   Experimental Evaluation

This section is structured as follows: we first describe the experiments on MNIST (along with the considered attacks and parameters for algorithms). We then discuss and experiment the limitations of the black-box setup we considered. We finally validate our take-aways on five large image classification models, in the last subsection of this evaluation.

We conduct experiments using the TensorFlow platform, using the Keras library.

4.1   Three neural networks for the MNIST dataset

The dataset used for those extensive experiments is the canonical MNIST database of handwritten digits, that consists of $60,000$ images as the training set, and of $10,000$ for the test set. The purpose of the neural networks we trained are of classifying images into one of the ten classes of the dataset.

The three off-the-shelf neural network architectures we use are available on the Keras website [3], namely as `mnist_mlp` (0.984% accuracy at 10 epochs), `mnist_cnn` (0.993% at 10) and `mnist_irnn` (0 .9918% at 900). We rename those into MLP, CNN and IRNN respectively. They constitute different characteristic architectures, with one historical multi-layer *perceptron*, a network with *convolutional* layers, and finally a network with *recurrent* units.
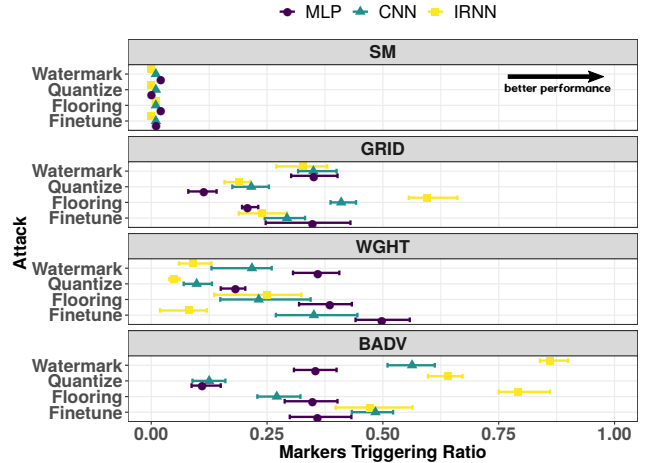

Figure 4: Performance results of the proposed algorithms (`GRID`, `WGHT` and `BADV`), with regards to the strawman approach (`SM`). Attacks applied to the models (listed on top) are indicated on the y-axis, while the ratio of triggered markers is indicated on the x-axis. Average results, as well as standard deviations for the algorithms are presented, the rightmost the better for their performance. For instance the `WGHT` algorithm, facing the fine-tuning attack, sees half of its key markers being triggered, while only one marker (ratio of $1/100$) is triggered for the strawman approach.

4.2   Attacks: from quantization to trojaning

This subsection lists the five attacks we considered. Excluding the watermarking and trojaning attacks, the others are standard operations over trained models; yet if an operator has already deployed its models on devices, any of those can be considered as attacks, as they tamper with the model that was designed for a precise purpose.

4.2.1   Quantization attack

This operation aims at reducing the number of bits representing each weight in the trained model. It is in practice widely used prior to deployment in order to fit the architecture and constraints of the target device. TensorFlow by default uses 32-bit floating points, and the goal is convert the model into 8-bit integers for instance. The TensorFlow `fake_quant_with_min_max_args` function is used to simulate the quantization of the trained neural network. We kept the default parameters of that func-

tion (8-bits quantization, with -6 to 6 as clamping range for the input).

4.2.2 Compression attack

A form of compression is *flooring*; it consists in setting to zero all model weights that are below a fixed threshold, and aims at saving storage space for the model. We set the following threshold value for the three networks: 0.0727, 0.050735 and 0.341 for the MLP, CNN and IRNN networks respectively. Those thresholds cause the degradation of network accuracies by about one percent (accuracies after the compression are 0.9749, 0.9829 and 0.9821, respectively).

4.2.3 Fine-tuning attack

Its consists in starting from a trained model, and to re-train it over a small batch of new data. This results in model weight changes, as the model was adapted through back-propagation to prediction errors made on that batch. We used a random sample of 300 inputs from the MNIST test set for that purpose.

4.2.4 Watermarking attack

Watermarking techniques [19, 23] embed information into the target model weights in order to mark its provenance. Since work in [19] operated on the MNIST dataset, and provided detailed parameters, we implemented this watermarking technique on the same models (MLP, CNN, and IRNN). The watermark insertion proceeds by fine-tuning the model over adversarial examples to re-integrate them into their original class, in order to obtain specific classifications for specific input queries (thus constituting a watermark). This approach requires a parameter for the mark that we set to 0.1, consistently with remarks made in [19] for maintaining the watermarked model accuracy.

4.2.5 Trojaning attack

We leverage the code provided in a GitHub repository, under the name of Stux-DNN, and that aims at trojaning a convolutional neural network for the MNIST dataset [4]. We first train the provided original model, and obtain an accuracy of 93.97% over the MNIST test set. The trojaning is also achieved with the provided code.

After applying those five attacks, the models accuracies changed; those are summarized on Table 2.

	MLP	CNN (Stux)	IRNN
Original model accuracy	0.9849	0.9932 (0.9397†)	0.9919
Quantization	0.9851	0.9928	0.9916
Flooring	0.9749	0.9829	0.9821
Fine-tuning	0.9754	0.9799	0.9917
Watermarking [19]	0.9748	0.9886	0.9915
Trojaning L0 [4]	-	(0.9340†)	-
Trojaning mask [4]	-	(0.9369†)	-

Table 2: Original model accuraries (white row), and accuracies resulting from attacks (grey rows). The lower the loss in accuracy, the stealthier the attack. Values marked † are obtained on the trojaned CNN model introduced in [4], and publicly available on the authors website.

Note that some attacks may surprisingly result in a slight accuracy improvement, as this is the case for MLP and quantization.

4.3 Algorithms settings

4.3.1 Settings for SM

SM uses a sample of images from the original MNIST test set, selected at random.

4.3.2 Settings for GRID

We use the Python Numpy uniform random generator for populating markers, that are images of 28x28 pixels.

4.3.3 Settings for WGHT

All the weights in the model are perturbed by adding to each of them a random float within $[-0.07, +0.07]$, $[-0.07, +0.07]$ or $[-0.245, +0.245]$ for the MLP, CNN and IRNN architectures respectively. This operation must keep the accuracy loss within a small percentage, while making it possible to cause enough classification changes for populating K (those values allowed to identify just over 100 markers).

4.3.4 Settings for BADV

For generating adversarial examples that are part of the key, we leverage the Cleverhans Python library [1]. The FGSM algorithm used in BADV, requires the ϵ parameter for the perturbation of inputs to *(i)* be small enough, and *(ii)* allow for the generation at least 200 adversarial examples out of $10,000$ files in the test set. ϵ is set to 0.04, 0.08 and 0.14 for the MLP, CNN and IRNN networks.

4.4 Experimental results

Results are presented in Figure 4, for all the attacks (excluding the trojaning attack), the three models and the four algorithms. We set key size $s = 100$; each experiment is executed 10 times.

`SM` generates markers that trigger with a probability below 0.02 for all attacks and all models; this means that some attacks such as for instance quantization over the MLP or IRNN models remain undetected after 100 query challenges.

All three proposed algorithms significantly beat that strawman approach; the most efficient algorithm, on average and in relative top-performances is `BADV`. Most notably, on the IRNN model it manages to trigger a ratio of up to 0.791 of markers, that is around 80% of them, for the flooring attack. This validates the intuition that creating sensitive markers from adversarial examples by the boundary (*i.e.*, with small ϵ values) is possible.

The third observation is that `GRID` arrives in second position for general performances: this simple algorithm, that operates solely on the data input space for generating markers, manages to be sensitive to boundary movements.

The `WGHT` algorithm has high performance peaks for the MLP model, with up to half of triggered markers for the fine-tuning attack, and a ratio of 0.385 for flooring (*i.e.*, more than one third of markers are triggered); it has the lowest performances of the three proposed algorithms, specifically for the IRNN model. This may come from the functioning of its recurrent architecture that makes it more robust to direct perturbations of weights: the model is more stable during learning (it requires around 900 epochs to be trained, while the two other models need only 10 epochs to reach their peak accuracy).

The watermark attack is very well detected on the IRNN model with the `BADV` algorithm (ratio of 0.86), on an equivalent rate on three models by `GRID`, while `SM` still shows trace amount of markers triggered for MLP and CNN, and none for IRNN.

Considering the relatively low degradation of the models reported on Table 2 (*i.e.*, within around 1% maximum)[2], we conclude that all three proposed algorithms capture efficiently the effects of even small attacks on the models to be defended, while `SM` would only be valuable in cases of large degradation of models. We illustrate in the subsection 4.6 the

---

[2]Trojaning attacks in [21] reports degradation over the original models of 2.60% (VGG Face recognition), 3% (speech recognition) or 3.50% (speech altitude recognition).
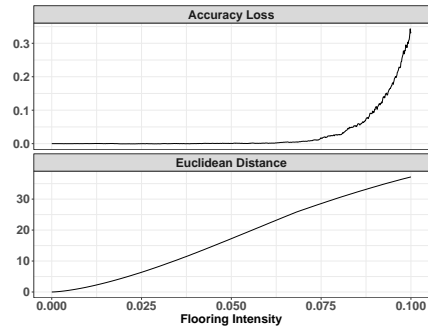
degradation-detectability trade-off.

Figure 5: Applying a compression (flooring) attack of increasing intensity (x-axis). Top-Figure: loss in accuracy of the attacked model, as compared to the original one. Bottom-Figure: measure of the Euclidean distance between the weights of the original and attacked models.
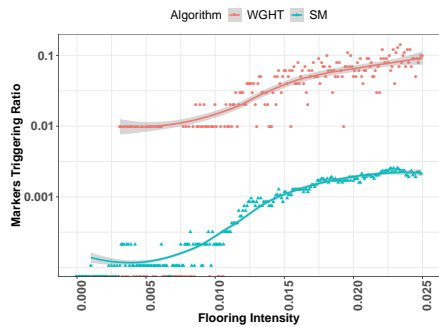

Figure 6: Impact of the same progressive flooring attack than in Figure 5 on the ratio of markers triggered for both `SM` and `WGHT` (y-axis, logscale).

4.5 Validation on a trojaning attack on MNIST

The modified accuracy of the neural network model proposed by [4], due to the attack, is reported on Table 2. The attack has two trojaning modes (L0 and mask). We now question the ability of one of our algorithms to also be outperforming the strawman approach `SM`; we experiment with `GRID`. Results are that `SM` manages to trigger ratios of 0.0524 and 0.0529 of markers, for L0 and mask modes respectively (please refer to their original paper for details on these techniques). `GRID` reaches ratios of 0.4560 and 0.4502, that are 8.7x and 8.5x increases in efficiency. This suggests that for a practical usage, a small key K of $s = 10$ will detect the attack, while `SM` is likely to raise a false negative.

4.6 Undetectable attacks and indistinguishably: illustrations

We now present examples that illustrate the inherent limits of a black-box interaction setup, as defined in subsection 2.1.

Let's consider the MLP model, along its best performing algorithm for tamper detection, `WGHT`. Assume that the model is tampered with using compression (flooring), and that we observe successive attacks: from an attack value (flooring threshold v) starting at 0, it reaches a value of $v = 0.1$ by increments of 0.001 (*i.e.*, at each attack, weights under v are floored). We observe the results after every attack; we plot in Figure 5 the loss in accuracy of the attacked model (top-Figure), and the Euclidean distance between the original and attacked model weights (bottom-Figure). For instance, we observe a 30% accuracy loss at a distance of 40. Since the loss is noticeable from around $v = 0.05$, we zoom in for plotting the corresponding ratio of markers triggered in Figure 6.

Those two figures convey two different observations, presented in the next two subsections.

4.6.1 Limits of the algorithms and of the black-box setup

The following cases may happen for attacks that have a very small impact on the model weights.

- *Case 1:* Accuracy changed after the attack, but the algorithm failed in finding at least one input that has changed class (*i.e.*, no marker from K has shown a classification change).

- *Case 2:* We did not manage to find any such input despite the attack.

Case 1 for instance occurs with $v = 0.004$, as seen in Figure 6. This means that both algorithms have failed, for the chosen key length s, to provide markers that were present in the zones where boundary moved due to the attack. (Please remind that, if the accuracy post attack has been modified, this means that some inputs from the test set has a changed label, then indicating that boundaries have de facto moved).

Case 2 is particularly interesting as it permits to illustrate Definition 3 in its restricted form: an attack occurred on $\mathcal{M}$ (as witness by a positive Euclidean distance between the two models in Figure 5), but it does not result in a measurable accuracy change.

It is α-set indistinguishable, with here α being the MNIST test set. We measure this case for $v = 0.003$, where pre and post accuracies are both 0.9849.

Case 1 motivates the proposal of new algorithms for the problem. We nevertheless highlight that the trojan attack [21] degrades the model on a basis of around 2%, while our algorithm is here unable to detect a tampering that is two order of magnitude smaller (accuracy loss of 0.02% for the attacked model). This indicate extreme cases for all future tampering detection approaches. *Case 2* questions the black-box interaction setup. This setup enables tampering detection in a lightweight and stealthy fashion, but may cause indecision due to the inability to conclude on tampering due to the lack of test data that can assess accuracy changes.

4.6.2 `WGHT` outperforms `SM` by nearly two orders of magnitude for small attacks

As observed in Figure 6, the `SM` markers triggered ratio ranges from 0.0001 to around 0.005, while for `WGHT` it ranges from 0.01 to 0.1, in this extreme case for attack detection with very low model degradation.

Figure 7 concludes this experiment by presenting the key size s that is to be chosen, depending on the algorithm and on the tolerance to attack intensity. This is in direct relation with the efficiency gap observed on previous figure: the more efficient the algorithm for finding sensitive markers, the smaller the query key for satisfying the according detection confidence. For an equivalent confidence, the key size to leverage for `SM` is 100 times longer than for the `WGHT` algorithm, confirming the efficiency of the techniques we proposed in this paper.

4.7 Validation on five large classifier models

We conducted extensive experiments on the standard MNIST dataset for it allows computations to run in a reasonable amount of time, due to the limited sizes of both its datasets and of the models for learning it. In order to validate the general claim of this paper, we now perform experiments on five large and recent models for image classification, using a state of the art dataset. This validation is interested in checking the consistency with the observation from the MNIST experiments, that have shown that our algorithms significantly outperform the strawman approach.
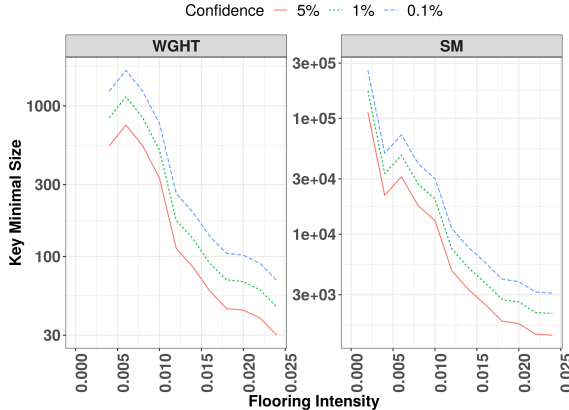
Figure 7: Key K size s (y-axis) to choose for a given challenge detection failure (noted confidence, on top-legend). Lines represent a smoothed average. Intuitively, the smaller the failure probability, the larger the key to select; this is the experimental counterpart to the analysis in Figure 2. Its size depends on the chosen algorithm and on the intensity of the flooring attack (x-axis).

We leverage five open-sourced and pre-trained models: VGG16 [31] (containing 138,357,544 parameters, as compared to MNIST models containing 669,706 (MLP), 710,218 (CNN) and 199,434 (IRNN) parameters), VGG19 [31] (143,667,240 parameters), ResNet50 [12] (25,636,712 parameters), MobileNet [14] (4,253,864 parameters) and DenseNet121 [15] (8,062,504 parameters). Except for the two VGG variants VGG16 and VGG19, all four architectures are broadly different models, that each were proposed as independent improvements for those image classification tasks (please refer to the Keras site [3] for each their own characteristics).

The VGGFace2 dataset has been made public recently [8]; it consists of a split of training (8631 labels) and test (500 labels) sets. The labels in the two sets are disjoint. We consider a random sample of 10,000 images of the VGGFace2 test dataset, for serving as inputs to the SM and WGHT algorithms. We note that despite that labels in the test set are different from the ones learnt in the models, this is a classic procedure (used *e.g.*, for experiments in work by Liu et al. [21]): a neural network with good performances will output stable features for new images, and thus in our case predict consistently the same class for each new given input. Those images are imported as 224x224 pixel images to query the tested models (versus 28x28 for MNIST). As for previous experiment (Figure 6), we experiment with the SM

and WGHT algorithms and $s = 100$, with the flooring attack. We perform the computations on four Nvidia TESLAs V100 with 32 Gb of RAM each; each setup is run three times and results are averaged (standard deviations are presented).

Figure 8 presents the results. The x-axis of each figure represents the flooring intensity, with the same values for all models, except for DenseNet because of its noticeable sensitivity to attacks. VGG16 corresponds to the neural network architecture of trojaned in paper [21]. For all models, we observe that an attack of 0.00001 is bellow what both SM and WGHT can detect (situation presented in Section 4.6). For the second smaller considered attack values on the x-axis, only WGHT manages to trigger markers; this constitutes another evidence that crafted markers are more sensitive and will trigger first for the smallest detectable attacks. For all the remaining flooring parameters, SM triggers markers, but always significantly less than WGHT (up a factor of 15 times less, at $x = 0.001$ on VGG19). All the models exhibit a very similar trend for both curves. The triggering ratio in the case of ResNet is lower for both WGHT and SM, while gap between the two approaches remains similar. Finally, in the DenseNet case, we note a higher triggering ratio for SM than for other models on the last three flooring values; the results are still largely in favor of the WGHT algorithm.

5   Related Work

Research works targeting the security of embedded devices such as IoT devices [29], suggest that traditional security mechanisms must be reconsidered. Main problems for traditional security tools is the difficulty to fix software flaws on those devices, the frequency to which those flows are reported, and finally their limited resources for the implementation of efficient protections.

Anti-tampering techniques for traditional software applications may be applied directly on the host machine in some defense scenarios. This is the case for the direct examination of the suspected piece of software [10]. *Remote attestation* techniques [9] allows for the distant checking of potential illegitimate modifications of software or hardware components; this is nevertheless requiring the deployment of a specific challenge/response framework (often using cryptographic schemes), that both parties should comply with. *Program result checking* (or black-box testing) is an old technique that inspects the compliance of a
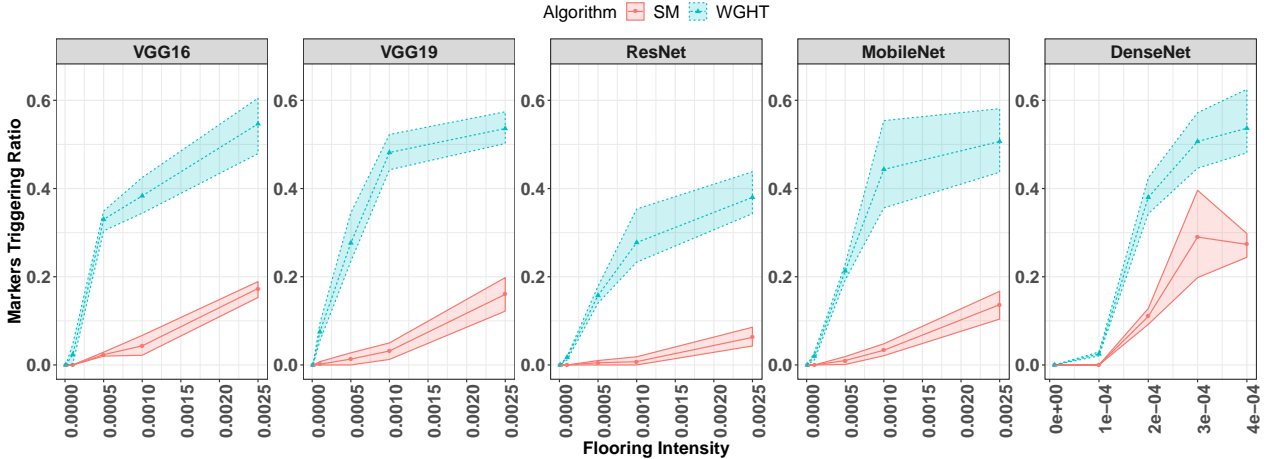
Figure 8: Marker triggering ratio for five large image classification models. One proposed algorithm (`WGHT`) versus the strawman approach (`SM`), facing the flooring attack. A sample of the VGGFace2 test dataset is used.

software by observing outputs on some inputs with expected results [7]; it has been applied in conventional software applications, but not on the particular case of deep learning models, where the actions are driven by an interpretation of a model (its weights in particular) at runtime. In that light, the work we proposed in this paper is a form of result checking for neural model integrity attestation. Since it is intractable to iterate over all possible inputs of a neural network model to fully characterize it (unlike for reverse engineering finite state machines [35] for instance), due to the dimensionality of inputs in current applications, the challenger is bound to create some algorithms to find some specific inputs that will carry the desired observations.

After a fast improvement of the results provided by neural network-based learning techniques in the past years, models found practical deployments into user devices [18]. The domain of security for those models is a nascent field [26], following the discovery of several types of attacks. The first one is the intriguing properties of adversarial attacks [6, 11, 17, 33] for fooling classifications; a wide range of proposals are attempting to circumvent those attacks [22, 25, 37]. Counter measures for preventing the stealing of machine learning models such as neural networks thought prediction APIs are discussed in [34]; it includes the recommendation for the service provider not to send probability vectors along with labels in online classification services. Some attacks are willing to leak information about individual data records that were used during the training of a model

[30, 32]; countermeasures are to restrict the precision of probability vectors returned by the queries, or to limit those vectors solely to top-k classes [30]. The possibility to embed information within the models themselves with watermarking techniques [19, 23] is being discussed on the watermark removal side by approaches like [13]. Trojaning attacks [4, 21] are yet not addressed, except by this paper, that introduced the problem and brought three novel algorithms to detect the tampering with models in a black-box setup.

6 Conclusion

Neural network-based models enable applications to reach new levels of quality of service for the end-user. Those outstanding performances are in balance, facing the risks that are highlighted by new attacks issued by researchers and practitioners. This paper introduced the problem of tampering detection for remotely executed models, by the use of their standard API for classification. We proposed algorithms that craft markers to query the model with; the challenger detects an attack on the remote model by observing prediction changes on those markers. We have shown a high level of performance as compared to a strawman approach that would use inputs from classic test sets for that purpose; the challenger can then expect to detect a tampering with very few queries to the remote model, avoiding false negatives. We believe that this application-level security checks, that operate at the model level and then at the granularity of the input data itself, is raising interesting futureworks for

the community.

While we experimented those algorithms facing small modifications made to the model by attacks, we have also shown that below a certain level of modification, the black-box setup may not permit to detect tampering attacks. In other situations, where the attack is observed in practice through accuracy change in the model, our algorithms can fail in the detection task. Some even more sensitive approaches might be proposed in the future. We believe this is an interesting futurework direction, that is to be linked with the growing understanding of the inner functioning of neural networks, and on their resilience facing attacks.

References

[1] Cleverhans code. `https://github.com/tensorflow/cleverhans`.

[2] Foolbox code. `https://github.com/bethgelab/foolbox/`.

[3] Keras code. `https://github.com/fchollet/keras/blob/master/examples/`.

[4] Stuxnnet. `https://github.com/Soldie/stux-DNN/`.

[5] Trojannn code. `https://github.com/PurduePAML/TrojanNN`.

[6] B. Biggio and F. Roli. Wild patterns: Ten years after the rise of adversarial machine learning. *Pattern Recognition*, 84:317 – 331, 2018.

[7] M. Blum. Program checking. In S. Biswas and K. V. Nori, editors, *Foundations of Software Technology and Theoretical Computer Science*, pages 1–9, Berlin, Heidelberg, 1991. Springer Berlin Heidelberg.

[8] Q. Cao, L. Shen, W. Xie, O. M. Parkhi, and A. Zisserman. Vggface2: A dataset for recognising faces across pose and age. In *FG*, 2018.

[9] G. Coker, J. Guttman, P. Loscocco, A. Herzog, J. Millen, B. O'Hanlon, J. Ramsdell, A. Segall, J. Sheehy, and B. Sniffen. Principles of remote attestation. *International Journal of Information Security*, 10(2):63–81, Jun 2011.

[10] C. S. Collberg and C. Thomborson. Watermarking, tamper-proofing, and obfuscation - tools for software protection. *IEEE Transactions on Software Engineering*, 28(8):735–746, Aug 2002.

[11] I. J. Goodfellow, J. Shlens, and C. Szegedy. Explaining and harnessing adversarial examples. In *ICLR*, 2015.

[12] K. He, X. Zhang, S. Ren, and J. Sun. Deep residual learning for image recognition. *CoRR, abs/1512.03385*, 2015.

[13] D. Hitaj and L. V. Mancini. Have you stolen my model? evasion attacks against deep neural network watermarking techniques. *CoRR*, abs/1809.00615, 2018.

[14] A. G. Howard, M. Zhu, B. Chen, D. Kalenichenko, W. Wang, T. Weyand, M. Andreetto, and H. Adam. Mobilenets: Efficient convolutional neural networks for mobile vision applications. *CoRR*, abs/1704.04861, 2017.

[15] G. Huang, Z. Liu, L. v. d. Maaten, and K. Q. Weinberger. Densely connected convolutional networks. In *CVPR*, 2017.

[16] T. Hwu, J. Isbell, N. Oros, and J. Krichmar. A self-driving robot using deep convolutional neural networks on neuromorphic hardware. In *IJCNN*, 2017.

[17] A. Kurakin, I. J. Goodfellow, and S. Bengio. Adversarial examples in the physical world. *CVPR*, 2017.

[18] N. D. Lane, S. Bhattacharya, P. Georgiev, C. Forlivesi, L. Jiao, L. Qendro, and F. Kawsar. Deepx: A software accelerator for low-power deep learning inference on mobile devices. In *IPSN*, 2016.

[19] E. Le Merrer, P. Perez, and G. Trédan. Adversarial frontier stitching for remote neural network watermarking. *CoRR*, abs/1711.01894, 2017.

[20] C. Lee and D. A. Landgrebe. Decision boundary feature extraction for neural networks. *IEEE Transactions on Neural Networks*, 8(1):75–83, Jan 1997.

[21] Y. Liu, S. Ma, Y. Aafer, W.-C. Lee, J. Zhai, W. Wang, and X. Zhang. Trojaning attack on neural networks. In *NDSS*, 2018.

[22] D. Meng and H. Chen. Magnet: A two-pronged defense against adversarial examples. In *CCS*, 2017.

[23] Y. Nagai, Y. Uchida, S. Sakazawa, and S. Satoh. Digital watermarking for deep neural networks. *IJMIR*, 7(1):3–16, Mar 2018.

[24] N. Papernot, P. McDaniel, I. Goodfellow, S. Jha, Z. B. Celik, and A. Swami. Practical black-box attacks against machine learning. In *ASIA CCS*, 2017.

[25] N. Papernot, P. McDaniel, X. Wu, S. Jha, and A. Swami. Distillation as a defense to adversarial perturbations against deep neural networks. In *S&P*, 2016.

[26] N. Papernot, P. D. McDaniel, A. Sinha, and M. P. Wellman. Towards the science of security and privacy in machine learning. *CoRR*, abs/1611.03814, 2016.

[27] O. M. Parkhi, A. Vedaldi, and A. Zisserman. Deep face recognition. In *BMVC*, 2015.

[28] K. Pei, Y. Cao, J. Yang, and S. Jana. Deepxplore: Automated whitebox testing of deep learning systems. In *SOSP*, 2017.

[29] J. Roux, E. Alata, G. Auriol, V. Nicomette, and M. Kaniche. Toward an intrusion detection approach for iot based on radio communications profiling. In *EDCC*, 2017.

[30] R. Shokri, M. Stronati, C. Song, and V. Shmatikov. Membership inference attacks against machine learning models. In *S&P*, 2017.

[31] K. Simonyan and A. Zisserman. Very deep convolutional networks for large-scale image recognition. *CoRR*, abs/1409.1556, 2014.

[32] C. Song, T. Ristenpart, and V. Shmatikov. Machine learning models that remember too much. In *CCS*, 2017.

[33] C. Szegedy, W. Zaremba, I. Sutskever, J. Bruna, D. Erhan, I. J. Goodfellow, and R. Fergus. Intriguing properties of neural networks. In *ICLR*, 2013.

[34] F. Tramer, F. Zhang, A. Juels, M. K. Reiter, and T. Ristenpart. Stealing machine learning models via prediction apis. In *USENIX Security*, 2016.

[35] N. Walkinshaw, K. Bogdanov, M. Holcombe, and S. Salahuddin. Reverse engineering state machines by interactive grammar inference. In *14th Working Conference on Reverse Engineering (WCRE 2007)*, pages 209–218, Oct 2007.

[36] B. Wu, F. N. Iandola, P. H. Jin, and K. Keutzer. Squeezedet: Unified, small, low power fully convolutional neural networks for real-time object detection for autonomous driving. *IEEE Conference on Computer Vision and Pattern Recognition Workshops (CVPRW)*, 2017.

[37] W. Xu, D. Evans, and Y. Qi. Feature squeezing: Detecting adversarial examples in deep neural networks. In *NDSS*, 2018.